MolecularLibraries
Pathways to Discovery

Probe Report

Title: Discovery and development of a second highly selective M_1 Positive Allosteric Modulator (PAM).
Authors: Thomas M. Bridges, Paul R. Reid, L. Michelle Lewis, Eric S. Dawson, C. David Weaver, Michael R. Wood, Craig W. Lindsley* (craig.lindsley@vanderbilt.edu)

Assigned Assay Grant #: MH077606-01
Screening Center Name & PI: Vanderbilt Screening Center for GPCRs, Ion Channels and Transporters, C. David Weaver
Chemistry Center Name & PI: Vanderbilt Specialized Chemistry Center for Accelerated Probe Development, Craig W. Lindsley
Assay Submitter & Institution: P. Jeffrey Conn, Vanderbilt University

PubChem Summary Bioassay Identifier (AID): 2543

Probe Structure & Characteristics:

2-((1-(5-bromo-2-fluorobenzyl)-1*H*-indol-3-yl)sulfonyl)-N-(5-methylisoxazol-3-yl)acetamide
MW = 506.4, logP = 3.9, TPSA = 94.2 Å^2

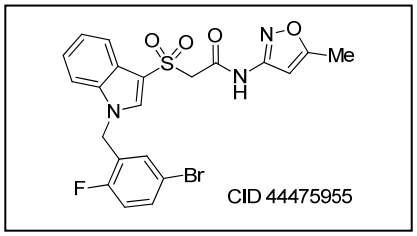

ML169

CID/ML#	Target Name	IC_{50}/EC_{50} (nM) [SID, AID]	Anti-target Name(s)	IC_{50}/EC_{50} (μM) [SID, AID]	Selectivity	Secondary Assay(s) Name: IC_{50}/EC_{50} (nM) [SID, AID]
44475955 ML169	M_1	1380 [85756541 , 2651]	M_2, M_3, M_4, M_5 Ricerca Lead Profiling	> 30 μM [85756541, 2430, 2428, 2438, 2433]	>30	ACh Fold-shift (45-fold) [85756541, 2434]

Recommendations for the scientific use of this probe:

This probe (CID 44475955) can be used for *in vitro* molecular pharmacology and electrophysiology experiments to study the receptor trafficking profile and the role of selective M_1 receptor activation by this unique M_1 PAM chemotype. Use of this probe alongside our initial M_1 PAM probe (CID 44251556) could improve our understanding of the M_1 signaling pathway and elucidate the difference, if any, between high and low ACh fold-shift compounds, due to their different pharmacological characteristics. This probe possesses high selectivity versus M_2-M_5, as well as a large panel of GPCRs, ion channels and transporters. While *in vivo* studies are possible, it has not been investigated for such uses.

Specific AIM: To identify small molecule positive allosteric modulators (PAMs) and/or allosteric agonists of the M_1 muscarinic acetylcholine receptor that are cell permeable, possess submicromolar potency and show greater than 10-fold selectivity over the other mAChRs (M_2-M_5) employing a functional HTS approach. Out of this effort aimed at M_1, which afforded a highly selective M_1 antagonist (CID 24768606), a highly selective M_1 allosteric agonist (CID 25010775) and a highly selective M1 PAM (CID 44251556), we also identified and optimized the first M_5 ligand, an M_5 PAM (CID 42633508). Starting from an unrelated lead, belonging to a novel chemotype, we have now been able to develop a second highly selective M_1 PAM with a low-micromolar EC_{50} and a greatly improved ACh fold-shift. Another MLSCN screening effort identified a highly selective M_4 PAM (CID 864492); thus, two MLSCN/MLPCN screens have provided a toolkit of highly selective mAChR ligands available from the MLPCN to study individual mAChR function both *in vitro* and *in vivo*.

Significance: The five cloned muscarinic acetylcholine receptor subtypes (mAChR1-5 or M_1-M_5) are known to play highly important and diverse roles in many basic physiological processes.[1-3] Correspondingly, muscarinic agonists and antagonists targeting one or more subtypes have been used preclinically and clinically for research and treatment of a wide range of pathologies.[3,4] Based on the high sequence homology of the mAChRs across subtypes, and particularly within the orthosteric acetylcholine (ACh) binding site, discovery of truly subtype-selective compounds has proven historically difficult. Due to the scarcity of selective compounds, a detailed understanding of the precise roles of each subtype in neurobiology and in various central nervous system (CNS) disorders has thus remained elusive.[3,4] In numerous Phase II and III clinical trials, pan-mAChR agonists were shown to improve cognitive performance in AD patients, but the GI-and/or cardiovascular side effects, resulting from activation of peripheral mAChRs, were deemed intolerable and the trials were discontinued.[5,6] Importantly, several pan-mAChR agonists demonstrated a decline in the concentration of Aβ42 in the cerebral spinal fluid of AD patients, suggesting that mAChR activation has the potential to be disease modifying as well as providing palliative cognitive therapy.[7] More recent studies in 3xTg-AD mice further support a disease modifying role for mAChR activation, and several Ph III trials demonstrated that mAChR activation lowered Aβ42 in patients.[8] Interestingly, the M_1/M_4 preferring xanomeline, in addition to improving cognitive performance, had robust therapeutic effects on the psychotic symptoms and behavioral disturbances associated with AD and recently published clinical trial data indicates efficacy in schizophrenic patients.[9,10] Probes developed from these efforts will greatly advance the current state of the art by aiding in the understanding of M_1's role in cell-based physiology and may extend the clinical understanding of psychotic and cognitive symptoms associated with neurodegenerative disorders like Alzheimer's Disease and schizophrenia.

Rationale: In recent years, major advances have been made in the discovery of highly selective agonists of other G protein-coupled receptors (GPCRs) that act at an allosteric site rather than the orthosteric binding site.[11,12] By screening for compounds that act at an allosteric site on the receptor, it is anticipated that compounds that selectively activate M_1 versus the other muscarinic subtypes may be identified.[13-18] While allosteric M_1 agonists have been identified, AC-42 and TBPB, they both suffer from undesirable ancillary pharmacology, poor physicochemical properties, poor pharmacokinetics and/or limited CNS exposure.[19,20] Thus, to truly enable the biomedical community to dissect the relative contributions of selective M_1 activation in preclinical models of AD and schizophrenia and to understand the role of M_1 in the pronounced efficacy of the M_1/M_4 preferring xanomeline,

improved M_1 probes are required. Recently, a number of novel highly subtype-selective allosteric ligands for M_1 and M_4 have emerged from functional cell-based screening efforts – several are MLPCN probes along with the prototypical M_1 PAM, BQCA.[13-18,20-22] Although considerable interest was initially generated around BQCA, this level of interest appears to have waned and may point to a fatal flaw in its general chemotype (See Figure 2). Our initial report on the discovery of CID 3008304, a pan G_q M_1, M_3, M_5 PAM, also described three other series of weak M_1 PAMs, and established that different M_1 PAM chemotypes displayed different modes of activity on downstream receptor signaling/trafficking despite similar profiles in Ca^{2+} assays.[13] Thus, all allosteric M_1 activation is not equivalent, and additional tool compounds representing diverse chemotypes are required to truly dissect and study M_1 function in the CNS. Subsequent to our development of an M_5 selective PAM from a pan G_q M_1, M_3, M_5 PAM,[21,22] we next optimized CID 3008304 for M_1 PAM activity resulting in the first highly selective M_1 PAM MLCPN probe (CID 44251556). For the above reasons associated with downstream receptor signaling/trafficking, we were simultaneously pursuing alternative leads in an attempt to add unique chemotypes to our tool kit of selective M_1 activators.[23]

Screening Center Information:
Assay Implementation and Screening
PubChem Bioassay Name: Discovery of Novel Allosteric Modulators of the M_1 Muscarinic Receptor: Positive Allosteric Modulator (PAM)

List of PubChem bioassay identifiers generated for this screening project (AIDs): 2651, 2425, 2428, 2430, 2434, 2433, 2438, 2626, and 2543.

PubChem Primary Assay Description: Chinese hamster ovary (CHO K1) cells stably expressing rat (r)M_1 were purchased from the American Type Culture Collection (ATCC, Manassas, VA) and cultured according to their recommendations. CHO cells stably expressing human (h) M_2, hM_3, and hM_5 were generously provided by A. Levey (Emory University, Atlanta, GA); rM_4 cDNA provided by T. I. Bonner (National Institutes of Health, Bethesda, MD) was used to stably transfect CHO-K1 cells purchased from the ATCC using Lipofectamine 2000. To make stable hM_2 and rM_4 cell lines for use in calcium mobilization assays, cell lines were cotransfected with a chimeric G protein (G_{qi5}) using Lipofectamine 2000. hM_2, hM_3, and hM_5 cells were grown in Ham's F-12 medium containing 10% heat-inactivated fetal bovine serum, 2 mM GlutaMax I, 20 mM HEPES, and 50 μg/mL G418 sulfate. hM_2-G_{qi5} cells were grown in the same medium supplemented with 500 μg/mL hygromycin B. Stable rM_4 cells were grown in Dulbecco's modified Eagle's medium containing 10% heat-inactivated fetal bovine serum, 2 mM GlutaMax I, 1 mM sodium pyruvate, 0.1 mM nonessential amino acids, 20 mM HEPES, and 400 μg/mL G418 sulfate; rM_4-G_{qi5} cells were grown in the same medium supplemented with 500 μg/mL hygromycin B. CHO cells stably expressing rM_1, hM_3, or hM_5 were plated at a seeding density of 50,000 cells/100 μL/well. CHO cells stably coexpressing hM_2/G_{qi5} and rM_4/G_{qi5} were plated at a seeding density of 60,000 cells/100 μL/well. For calcium mobilization, cells were incubated in antibiotic-free medium overnight at 37 °C/5% CO_2 and assayed the next day.

Calcium Mobilization Assay: Cells were loaded with calcium indicator dye [2 μM Fluo-4 acetoxymethyl ester (50 μL/well) prepared as a stock in DMSO and mixed in a 1:1 ratio with 10% Pluronic acid F-127 in assay buffer (1xHanks' balanced salt solution supplemented with 20 mM HEPES and 2.5 mM probenecid, pH 7.4)] for 45 min at 37 °C. Dye was removed and replaced with the appropriate volume of assay buffer. All compounds were serially diluted in assay buffer for a final 2x stock in 0.6% DMSO. This stock was then added to the assay plate for a final DMSO concentration of 0.3%. Acetylcholine (EC_{20} concentration or full dose-response curve) was prepared at a 10x stock solution in assay buffer before addition to assay plates. Calcium mobilization was measured at 25 °C using a FLEXstation II (Molecular Devices, Sunnyvale, CA). Cells were preincubated with test compound (or vehicle) for 1.5

min before the addition of the agonist, acetylcholine. Cells were then stimulated for 50 s with a submaximal concentration (EC_{20}) or a full dose-response curve of acetylcholine. The signal amplitude was first normalized to baseline and then as a percentage of the maximal response to acetylcholine.

Center Summary of Screen: This screen was performed in the pilot phase, the MLSCN, when the MLSMR compound collection at Vanderbilt only contained ~65,000 compounds. Results from the primary M_1 screen of these compounds identified ~12 putative M_1 PAMs with an average Z' score of 0.70±0.09. The confirmation screen (singles at 10 μM) produced two lead compounds, one of which was optimized into our first M_1 PAM probe (CID 44251556). The other, CID 2157678, represented a viable lead structure already endowed with good receptor subtype selectivity across the M_3/M_5 receptors (**Figure 1**). However, its potency upon reconfirmation from dry solid (M_1 EC_{50} = 12.9 μM) was not particularly attractive and so a program was initiated to develop this lead into a pharmacologically more useful tool by improving its potency while maintaining its M_2-M_5 receptor subtype selectivity. Ultimately, it was envisioned that an M_1 PAM not structurally related to the known M_1 PAMs (CID 44251556 and BQCA, **Figure 2**) may possess a distinct pharmacology at the M_1 receptor, thereby enabling an expanded understanding of the M_1 muscarinic receptor's downstream signaling/trafficking.

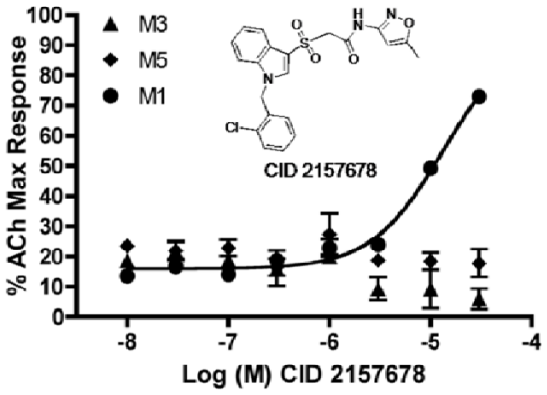

Figure 1. CRCs at M_1-M_5 for HTS lead CID 2157678.

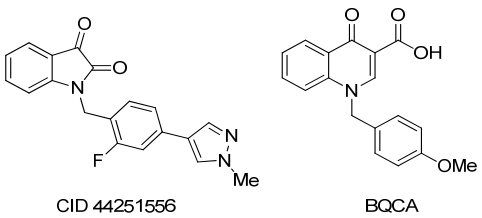

Figure 2. M_1 PAMs, CID 44251556 and BQCA

Probe Chemical Lead Optimization Strategy: Our initial optimization strategy is outlined in Figure 3, and as SAR with allosteric ligands is often shallow, we employed an iterative parallel synthesis approach, along with targeted syntheses for structures encompassing more speculative modifications. Attempted modifications of the Eastern oxazole-amide, although not extensive, met with no success, returning only compounds with undetectable activity (Such as CID 44129586, 44634499, 44634501 and 44634503). In a straightforward attempt to reduce molecular weight the benzyl group attached to the indole nitrogen was omitted, but met with a similar lack of success (CID 751482, EC_{50} > 10 μM).

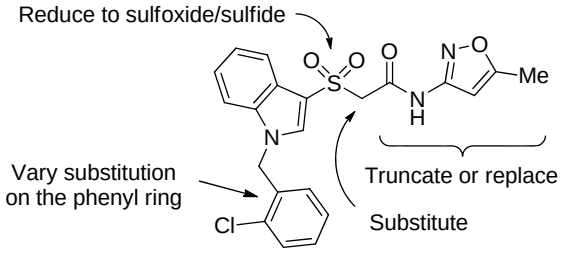

Figure 3. Initial optimization strategy for CID 2157678.

Scheme 1. Synthesis of CID 2157678 and the route to its analogs.

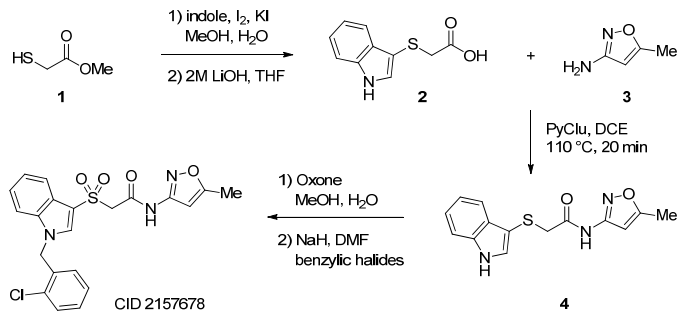

Accordingly, libraries were concomitantly prepared as shown in Scheme 1 and predominately surveyed diversity on the Southern benzyl moiety. Methyl thioglycolate (**1**) was arylated with indole using iodine and potassium iodide, followed by saponification of the ester using

lithium hydroxide to give acid **2**. This acid was then peptide coupled with 3-amino-5-methyl-isoxazole (**3**) employing PyClU (chlorodipyrrolidinocarbenium hexafluorophosphate), in DCE, with microwave heating to yield thioether **4**. The sulfur was then oxidized to the sulfone with Oxone, thereby allowing the benzylation of the indole nitrogen to be performed as the final step in the preparation of the initial library (Analogs **5**, **Table 1**). As would be expected for this benzylation, bis-alkylation was observed to a small extent, and occasionally allowed for the isolation of analogs like CID 44129599 (**Figure 4**). While it was not terribly surprising that these analogs were devoid of M_1 PAM activity, it would eventually be ascertained that even the introduction of a solitary methyl group α to the amide abolished any measureable M_1 PAM activity (CID 44634500, M_1 EC_{50} > 10 μM, is the α-methylated analog of the probe compound). Alternatively, if the Oxone oxidation step is omitted or replaced with a milder oxidant (e.g. $FeCl_3/H_5IO_6$) then thioethers (CID 3305286) or sulfoxides (CID 44247543) analogous to the lead structure were produced. However only the sulfoxide (CID 44247543) retained measureable activity (M_1 EC_{50} = 5.23 μM), but did not represent a significant improvement over its sulfone analog (**5b**, CID 44129591, **Table 1**).

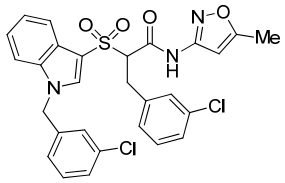

CID 44129599

Figure 4. A representative over-alkylation product from **Scheme 1**.

Focusing on the library of analogs appearing in Table 1, we quickly discovered that substitution in the 3-position of the phenyl ring was preferred. Moving the chlorine from the 2-position in the lead structure (**5a**) to the 3-position (**5b**) improved the M_1 EC_{50} by about 50%. While, either a methoxy (**5e**) or a fluorine (**5f**) at this position afforded a small improvement in their EC_{50} values, a 2-fold increase in potency could be obtained by introducing a bromine at the 3-position providing **5h**, which possessed an EC_{50} = 3.79 μM. The remainder of Table 1, servers to illustrated how steep the SAR was for this class of allosteric modulators. For example, the addition of a second halogen in examples **5k** and **5l** eliminated the measurable efficacy displayed by their mono-halogenated analogs (**5h** and **5b**, respectively). In general it could also be concluded that substitution at the 4-position on these aryl groups was uniformly detrimental. Having learned from the initial library that proper substitution at the 3-position of the benzyl group could be beneficial, and with the bromide **5h** in hand we sought to introduce various aryl rings at this location. The small library of analogs **6** appearing in Table 2 were prepared via microwave-assisted Suzuki couplings between **5h** and the requisite boronic acid. Impetus for the introduction of the pyrazole moiety found in **6a-c**, came from its successful incorporation into our previous M_1 PAM probe (CID 44251556) and BQCA analogs (**Figure 2**). Gratifyingly, the *N*-methyl pyrazole **6a** did have measureable activity but did not impart

Table 1. Structures and activities of analogs **5**.

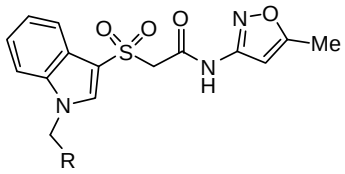

Cmpd	CID	R	M_1 EC_{50} (μM)	%ACh Max
5a	2157678	2-Cl phenyl	9.71	83
5b	44129591	3-Cl phenyl	5.82	96
5c	2157657	4-Cl phenyl	> 10	-
5d	44129592	2-OMe phenyl	> 10	-
5e	44129593	3-OMe phenyl	6.54	79
5f	44129594	4-OMe phenyl	> 10	-
5g	2157612	3-F phenyl	5.22	96
5h	44247542	3-Br phenyl	3.79	91
5i	44241483	3-CF_3 phenyl	> 10	-
5j	44241487	3-CN phenyl	> 10	-
5k	44634502	3,5-diBr phenyl	> 10	-
5l	44241486	3,4-diCl phenyl	> 10	-
5m	44129587	4-CF_3 phenyl	> 10	-
5n	44129588	4-OCF_3 phenyl	> 10	-
5o	44129590	2-F phenyl	> 10	-
5p	44129589	2,4-diF phenyl	> 10	-
5q	44129585	2-Br-4-F phenyl	> 10	-
5r	44216760	6-F pyridin-3-yl	> 10	-

a significant improvement in potency over the corresponding bromide (**5h**). Divergent from the SAR established during the development of CID 44251556, the unalkylated pyrazole **6b** was now preferred, possessing an M_1 EC_{50} = 2.19 µM. In contrast to the *N*-methyl pyrazole **6a**, the larger *sec*-butyl substituent of **6c** was not tolerated, and neither were the other heterocycles of the remaining analogs (**6d-h**).

To further the development of this novel series of M_1 PAMs we focused on three of the more potent analogs (**5b**, **5h** and **6b**) and applied a fine-tuning process of introducing fluorine atoms at various locations to provide analogs **7** (**Table 3**). Across the series, substitution at the 4-position was uniformly not tolerated (**7a-c**), consistent with the SAR appearing in Table 1. Bis-fluorination of the indole ring eroded activity in the context of the bromine analog **7d** but conversely augmented the activity of the pyrazole congener **7e**. This type of subtle/confounding SAR was similarly observed with respect to fluorination at the R^2 position in analogs **7f-h**. While the presence of a fluorine at R^2 was neutral or slightly beneficial in the context of the chlorine analog (**7f**), its presence resulted in clearly decreased activity for both the bromine and pyrazole analogs, **7g** and **7h**. Lastly, the introduction of a single fluorine at the R^6 position could either be moderately detrimental in the context of pyrazole **7i** or decidedly beneficial with respect to bromine analog **7j**, where an almost 3-fold improvement in potency was observed. In this manner, both CID 44475955 (**7j**) and the related difluorindole analog CID 44475948 (**7e**) were developed and chosen for further evaluation (For clarity, these compounds are shown in Figure 5).

Table 2. Structures and activities of analogs **6**.

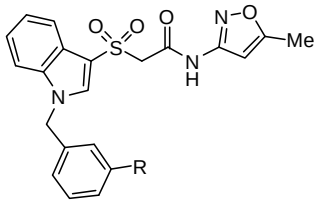

Cmpd	CID	R	M_1 EC_{50} (µM)	%ACh Max
6a	44247543	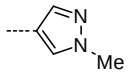	3.21	102
6b	44216758	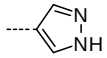	2.19	90
6c	44475951	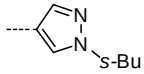	> 10	-
6d	44241482	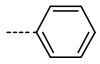	> 10	-
6e	44216757	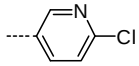	> 10	-
6f	44475953	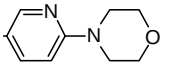	> 10	-
6g	44475954	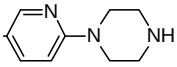	> 10	-
6h	44475952	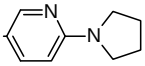	> 10	-

Table 3. Structures and activities of analogs **7**.

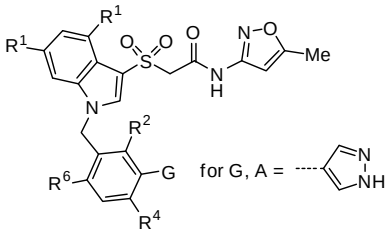

Cmpd	CID	G	R^1	R^2	R^4	R^6	M_1 EC_{50} (µM)	%ACh Max
7a	44475949	A	H	H	F	H	> 10	-
7b	44216756	Br	H	H	F	H	> 10	-
7c	44241484	Cl	H	H	F	H	> 10	-
7d	44475946	Br	F	H	H	H	5.37	103
7e	44475948	A	F	H	H	H	1.85	102
7f	44241485	Cl	H	F	H	H	5.10	56
7g	44475947	Br	H	F	H	H	> 10	-
7h	44475450	A	H	F	H	H	4.40	103
7i	44475956	A	H	H	H	F	3.07	96
7j	44475955	Br	H	H	H	F	1.38	84

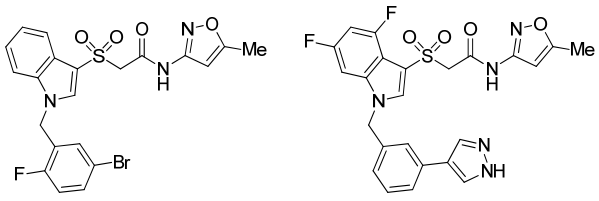

CID 44475955 (**7j**)
M_1 EC_{50} = 1.38 µM

CID 44475948 (**7e**)
M_1 EC_{50} = 1.85 µM

Figure 5. The two most potent M_1 PAMs developed from the lead CID 2157678.

Both CID 44475955 and CID 44475948 were highly selective PAMs for the M_1 receptor, displaying minimal/no potentiation of the M_2-M_5 receptors up to 30 µM (**Figure 6A-B**). Similarly, both compounds demonstrated impressive left-ward shifts in the potency of ACh in M_1 ACh Concentration Response Curve (CRC) fold-shift experiments (**Figure 6C**). When tested at 30 µM, the bromine analog **7j** engendered a 45-fold increase in ACh activity, while the pyrazole analog **7e** increased ACh activity 98-fold. These levels of

potentiation are very similar to those seen for BQCA[14,15] and represent a sizable improvement over the earlier M_1 PAM probe molecule CID 44251556 which produced only a 3-fold shift in an identical experiment. Still, these experiments did not reveal a definitive superiority for either molecule.

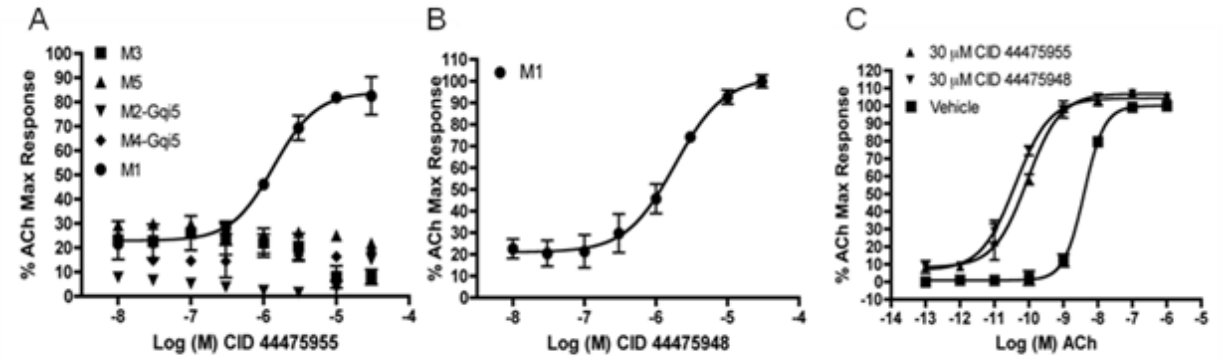

Figure 6. A) CRCs for CID 44475955 at M_1-M_5; B) CRCs for CID 44475948 at M_1-M_5; C) Fold-Shift for CID 44475955 and CID 44475948 at 30 μM.

An examination of calculated physical properties and practical considerations were more helpful in choosing the preferred probe. The *in silico* values for CID 44475955 and CID 44475948 appearing in Table 4 were calculated using TRIPOS software. Also included in Table 4 are the averages from the MDDR database of compounds both entering Phase I and launched drugs. Once again both compounds were very similar across a number of parameters. However, CID 44475955 possessed superior values for both total polar surface area (TPSA) and its number of hydrogen bond donors (Hdon). These two discrepancies both point to a lower probability of crossing the blood brain barrier for CID 44475948. Although not tested *in vivo*, this would lead to the prediction that CID 44475955 has a better chance of being a CNS penetrant molecule, and therefore a potentially superior MLPCN probe compound for the muscarinic receptors present in the CNS. Additionally, from a synthesis standpoint, the greater ease and lower cost for the acquisition of indole (**Scheme 1**) over 4,6-difluoroindole (the starting material for CID 44475948) makes CID 44475955 the more practical and cost-effective probe molecule.

To more fully characterize this novel M_1 PAM, CID 44475995 was tested at Ricerca's (formerly MDS Pharma's) Lead Profiling Screen (binding assay panel of 68 GPCRs, ion channels and transporters screened at 10 μM), and was, thus far, found to not significantly interact with 16 out of the 16 assays conducted (Remaining 52 pending).[24] Thus, CID 44475955 is highly selective and can be used to dissect the role of M_1 *in vitro*. Furthermore, when used in conjunction with our earlier M_1 PAM probe molecule, the potentially different effects caused by an ACh low fold-shift probe (CID 44251556, 3-fold) versus those of an ACh high fold-shift probe (CID 44475955, 45-fold) may reveal the importance of this parameter towards the treatment of different disease states.

Table 4: Calculated Property Comparison with MDDR Compounds

Property	CID44475955	CID 44475948	MDDR Phase I	MDDR Launched
MW	506.3	511.5	438.98	415.20
cLogP	3.92	3.24	3.21	2.21
TPSA	94.20	122.88	97.06	91.78
Hdon	1	2	2.12	2.13
Hacc	7	9	7.06	6.47
LogS	-7.18	-8.00	-4.96	-3.73
NrotB	5	6	7.08	5.71

In summary, from an initial MLSCN screening campaign of just 65,000 compounds a

second, potent and highly selective M_1 PAM (CID 44475955) has been identified which is structurally distinct from our initial M_1 PAM probe (CID 44251556). CID 44475955, similar to our previous probe, possesses comparable potency to BQCA, but now in contrast to our first probe, also shares BQCA's ability to produce a large left-ward shift in the activity of ACh at the M_1 receptor. CID 44475955 now represents the third known chemotype to provide potent and selective M_1 positive allosteric modulation. Further *in vitro* and *in vivo* characterization of CID 44475955 is in progress in the assay submitter's lab, and data will be reported in due course.

Synthetic procedure and spectral data for CID 44475955.

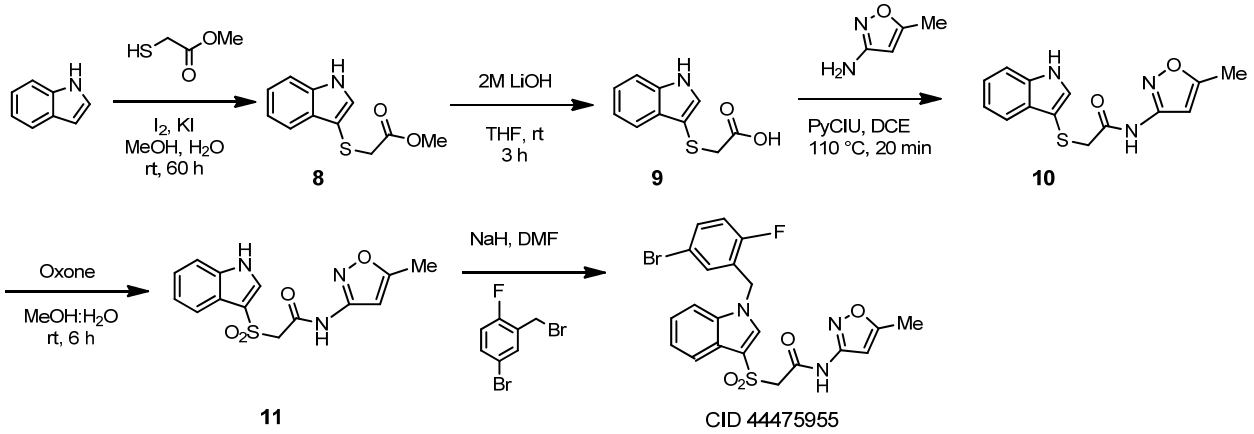

CID 44475955, 2-((1-(5-bromo-2-fluorobenzyl)-1*H*-indol-3-yl)sulfonyl)-*N*-(5-methylisoxazol-3-yl)acetamide [ML169]. To a solution of indole (3.00 g, 25.6 mmol) and methyl thioglycolate (2.40 mL, 25.6 mmol) in methanol:water (80 mL : 20 mL) was added iodine (6.50 g, 25.6 mmol) and potassium iodide (4.25 g, 25.6 mmol). The reaction mixture was stirred at ambient temperature for 60 hours. Methanol was removed *in vacuo* and the aqueous layer diluted with a saturated solution of sodium bicarbonate and extracted with ethyl acetate. The organic layer was dried over magnesium sulfate, evaporated *in vacuo* and the resulting residue was purified on a silica gel column (0-100% ethyl acetate:hexanes over 33 min) to afford compound **8** as an oil (LCMS >98%). Compound **8** was dissolved in a mixture of tetrahydrofuran (20 mL) and 2.0M aqueous LiOH (15 mL), then stirred vigorously at ambient temperature for 30 minutes. Tetrahydrofuran was removed *in vacuo*, the aqueous layer neutralized with 1.2 N HCl and extracted with CH_2Cl_2. The organic layer was dried over magnesium sulfate and removed *in vacuo* to produce an oily residue. Upon diluting the residue in dichloromethane a reddish-brown solid formed which was filtered and dried to yield compound **9** (2.00 grams, 9.65 mmol, 38% yield over 2 steps, LCMS >98%).

Compound **9** (650 mg, 3.14 mmol), 3-amino-5-methyl-isoxazole (616 mg, 6.28 mmol), PyClU (2.00 g, 6.28 mmol), and DIEA (1.36 mL, 7.85 mmol) were added to dichloroethane (25 mL) and microwave irradiated at 110 °C for 20 minutes. After cooling, the solvent was removed *in vacuo* and the remaining residue purified on a silica gel column (0-70% ethyl acetate:hexanes over 33 min) to yield compound **10** (642 mg, 2.23 mmol, 71% yield, LCMS >98%). Compound **10** (502 mg, 1.77 mmol) was dissolved in 25 mL (9:1, methanol:water) and Oxone (10.0 g, 17.7 mmol) was added. Stirring at ambient temperature continued overnight. Water (20 mL) was added and the mixture extracted with ethyl acetate (3x20 mL). The organics were combined, dried over magnesium sulfate, and concentrated *in vacuo* to give an oily residue which was purified on silica gel (0-50% ethyl acetate:hexanes over 19 min) to yield compound **11** (500 mg, 1.57 mmol, 88% yield, LCMS >98%). In a 5 mL microwave vial, compound **11** (55.0 mg, 0.174 mmol) was dissolved in DMF (3 mL) and cooled to 0 °C. Sodium hydride (60% by weight, 14.0 mg,

0.348 mmol) was then added in one portion and the reaction mixture vigorously stirred at 0 °C for 15 minutes. 4-bromo-2-bromomethyl-1-flouro-benzene (51.0 mg, 0.191 mmol) was added in one portion and the reaction mixture was stirred while being allowed to warm to ambient temperature over 3 hours. The reaction mixture was quenched with water (2 mL) and the solution was extracted with ethyl acetate (3x4 mL). The combined organics were dried over magnesium sulfate, concentrated *in vacuo* to give an oily residue which was purified on silica gel (0-70% ethyl acetate:hexanes over 19 min) to yield **CID 44475955** (45 mg, 0.088 mmol, 51% yield). LCMS >98% 214 nm, R_T = 1.34 min, m/z = 506 ([^{79}Br]m+1), 508 ([^{81}Br]m+1). ^{1}H NMR (400 MHz, DMSO-d_6) 11.27 (s, 1H), 8.23 (s, 1H), 7.82 (d, *J* = 8.0 Hz, 1H), 7.63 (d, *J* = 8.0 Hz, 1H), 7.56-7.58 (m, 1H), 7.47 (dd, *J* = 2.4 Hz, 6.4 Hz, 1H), 7.35-7.23 (m, 3H), 6.54 (s, 1H), 5.62 (s, 2H), 4.43 (s, 2H), 2.37 (s, 3H), HRMS found: 506.0184; calculated for $C_{21}H_{17}BrFN_3O_4S$: 506.0185.

MLS#s: 002700179 (Probe, 500 mg), 002700180, 002700181, 002700182, 002700183, 002700184

Bibliography

(1) Bonner, T.I.; Buckley, N.J.; Young, A.C.; Brann, M.R. *Science* **1987**, *237*, 527-532.
(2) Bonner, T.I.; Young, A.C.; Brann, M.R.; Buckley, N.J. *Neuron* **1988**, *1*, 403-410.
(3) Wess, J. *Annu. Rev. Pharmacol. Toxicol.* **2004**, *44*, 423-450.
(4) Langmead, C.J.; Watson, J.; Reavill, C. *Pharmacol. Ther.* **2008**, *117*, 232-243.
(5) Eglen, R.M.; Choppin, A.; Dillon, M.P.; Hedge, S. *Curr. Opin. Chem. Biol.* **1999**, *3*, 426-432.
(6) Felder, C.C.; Bymaster, F.P.; Ward, J.; DeLapp, N. *J.Med. Chem.* **2000**, *43*, 4333-4353.
(7) Bodick, N.C.; Ofen, W.W.; Levey, A.I.; Cutler, N.R.; Gauthier, S.G.; Satlin, A.; Shannon, H.E.; Tollefson, G.D.; Rasmussen, K.; Bymster, F.P.; Hurley, D.J.; Potter, W.Z.; Paul, S.M. *Arch. Neurol.* **1997**, *54*, 465-473.
(8) Caccamo, A.; Oddo, S.; Billings, L.M.; Green, K.N.; Martinez-Coria, H.; Fisher, A.; LaFerla, F.M. *Neuron* **2006**, *49*, 671-682.
(9) Fisher, A. *Neurodegener. Dis.* **2008**, *5*, 237–240.
(10) Shekhar, A., Potter, W. Z., Lightfoot, J., Lienemann, J., Dube, S., Mallinckrodt, C., Bymaster, F. P., McKinzie, D. L., and Felder, C. C. *Am. J. Psychiatry* **2008**, *165*, 1033–1039.
(11) Conn, P.J.; Christopoulos, A.; Lindsley, C.W. *Nat. Rev. Durg Disc.* **2009**, *8*, 41-54.
(12) Bridges, T.M.; Lindsley, C.W. *ACS Chem. Biol*. **2008**, *3*, 530-542.
(13) Marlo, J.E.; Niswender, C.M.; Days, E.L.; Bridges, T.M.; Xiang, Y.; Rodriguez, A.L.; Shirey, J.K.; Brady, A.E.; Nalywajko, T.; Luo, Q.; Austin, C.A.; Williams M.B.; Kim, K.; Williams, R.; Orton, D.; Brown, H.A.; Lindsley, C.W.; Weaver, C.D.; Conn, P.J. *Mol. Pharmacol.* **2009**, *75*, 577-588.
(14) Ma, L.; Seager, M.; Wittman, M.; Bickel, N.; Burno, M.; Jones, K.; Graufelds, V.K.; Xu, G.; Pearson, M.; McCampbell, A.; Gaspar, R.; Shughrue, P.; Danzinger, A.; Regan, C.; Garson, S.; Doran, S.; Kreatsoulas, C.; Veng, L.; Lindsley, C.W.; Shipe, W.; Kuduk, S.; Jacobson, M.; Sur, C.; Kinney, G.; Seabrook, G.R.; Ray, W.J. *Proc. Natl. Acad Sci. USA* **2009**, *106*, 15950-15955.
(15) Shirey, J.K.; Brady, A.E.; Jones, P.J.; Davis, A.A.; Bridges, T.M.; Jadhav, S.B.; Menon, U.; Christain, E.P.; Doherty, J.J.; Quirk, M.C.; Snyder, D.H.; Levey, A.I.; Watson, M.L.; Nicolle, M.M.; Lindsley, C.W.; Conn, P.J. *J. Neurosci*. **2009**, *29*, 14271-14286.
(16) Yang, F.V.; Shipe, W.D.; Bunda, J.L.; Nolt, M.B.; Wisnoski, D.D.; Zhao, Z.; Barrow, J.C.; Ray, W.J.; Ma, L.; Wittman, M.; Seager, M.; Koeplinger, K.; Hartman, G.D.; Lindsley, C.W. *Bioorg. Med. Chem. Lett*. **2010**, *20*, 531-536.
(17) Lebois, E.P.; Bridges, T.M.; Dawson, E.S.; Kennedy, J.p.; Xiang, Z.; Jadhav, S.B.; Yin, H.; Meiler, J.; Jones, C.K.; Conn, P.J.; Weaver, C.D.; Lindsley, C.W. *ACS*

Chemical Neurosci. **2010**, *1*, 104-121.
(18) Spalding, T.A.; Trotter, C.; Skajaerbaek, N.; Messier, T.L.; Currier, E.A.; Burstein, E.S.; Li, D.; Hacksell, U.; Brann, M.R. *Mol. Pharm*. **2002**, *61*, 1297-1302.
(19) Jones, C. K., Brady, A. E., Davis, A. A., Xiang, Z., Bubser, M., Tantawy, M. N., Kane, A. S., Bridges, T. M., Kennedy, J. P., Bradley, S. R., Peterson, T. E., Ansari, M. W., Baldwin, R. M., Kessler, R. M., Deutch, A. Y., Lah, J. J., Levey, A. I., Lindsley, C. W., and Conn, P. J. *J. Neurosci.* **2008**, *28*, 10422–10433.
(20) Brady, A.; Jones, C.K.; Bridges, T.M.; Kennedy, P.J.; Thompson, A.D.; Breininger, M.L.; Gentry, P.R.; Yin, H.; Jadhav, S.B.; Shirey, J.; Conn, P.J.; Lindsley, C.W. *J. Pharm. & Exp. Ther.* **2008**, *327*, 941-953.
(21) Bridges, T.M.; Marlo, J.E.; Niswender, C.M.; Jones, J.K.; Jadhav, S.B.; Gentry, P.R.; Weaver, C.D.; Conn, P.J.; Lindsley, C.W. *J. Med. Chem.* **2009**, *52*, 3445-3448.
(22) Bridges, T.M.; Kennedy, J.P.; Cho, H.P.; Conn, P.J.; Lindsley, C.W. *Bioorg. Med. Chem. Lett.* **2010**, *20*, 558-562.
(23) Bridges, T.M.; Kennedy, J.P.; Cho, H.P.; Conn, P.J.; Lindsley, C.W. *Bioorg. Med. Chem. Lett., in press.*
(24) For information on the Ricerca (formerly MDS Pharma) Lead Profiling Screen see: https://pharmacology.ricerca.com/Catalog/

APPENDIX I

Solubility, Stability and Reactivity data as determined by Absorption Systems

Solubility. Solubility in PBS (at pH = 7.4) for ML 169 was 0.08 μM.

Stability. Stability (at room temperature = 23 °C) for ML 169 in PBS (no antioxidants or other protectorants and DMSO concentration below 0.1%) is shown in the table below. After 48 hours, the percent of parent compound remaining was not reported, but the assay variability over the course of the experiment ranged from a low of 89% (at 15 minutes) to a high of 142% (at 1 hour).

	Percent Remaining (%)						
Compound	**0 Min**	**15 Min**	**30 Min**	**1 Hour**	**2 Hour**	**24 Hour**	**48 Hour**
ML 169	100	89	99	142	91	103	---

Reactivity. As assessed through a glutathione (GSH) trapping experiment in phosphate buffered saline (with a substrate concentration of typically 5-50 μM and a GSH concentration of 5 mM, at t = 60 minutes) ML 169 was found to not form any detectable GSH adducts.*

* Solubility (PBS at pH = 7.4), Stability and Reactivity experiments were conducted at Absorption Systems. For additional information see: https://www.absorption.com/site

APPENDIX II

Liquid Chromatography-Mass Spectrometry (LCMS)
and
Nuclear Magnetic Resonance (NMR)

as prepared by Vanderbilt Specialized Chemistry Center

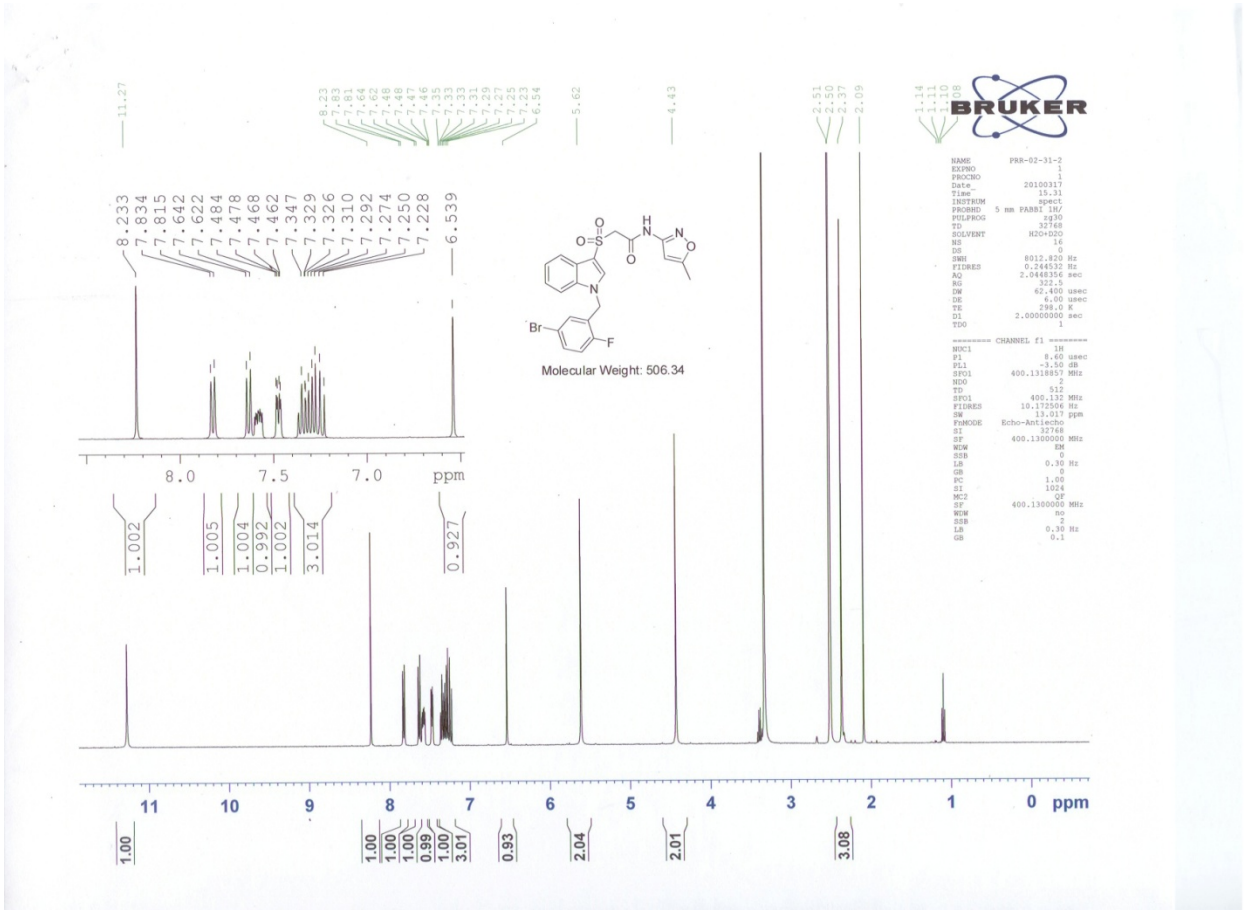
BRUKER
Molecular Weight: 506.34
ppm

MS Report

```
File ..EZXDATA\PAUL\03-10\PRR-02-31-111AGILENT 2.D Tgt Mass (EZX): 506.00
Injection Date    : 17 Mar 10   3:40 pm -0600          Seq. Line : 0
Sample Name       : PRR-02-31-1                    Location  : P2-E-01
Acq. Operator     : Paul Reid                          Inj : 1
Spec. Reported    : MS Integration                 Inj Volume : 3 ul
Acq. Method       : C:\Chem32\1\METHODS\ULTRA2_AQUEOUS.M
Analysis Method   : C:\Chem32\1\METHODS\ULTRA2_AQUEOUS.M
Sample Info : 506.00
Method Info : Restek Ultra II Aqueous C18 3.0x30mm 3u 10-100% ACN:H2O
(0.1%TFA)
```

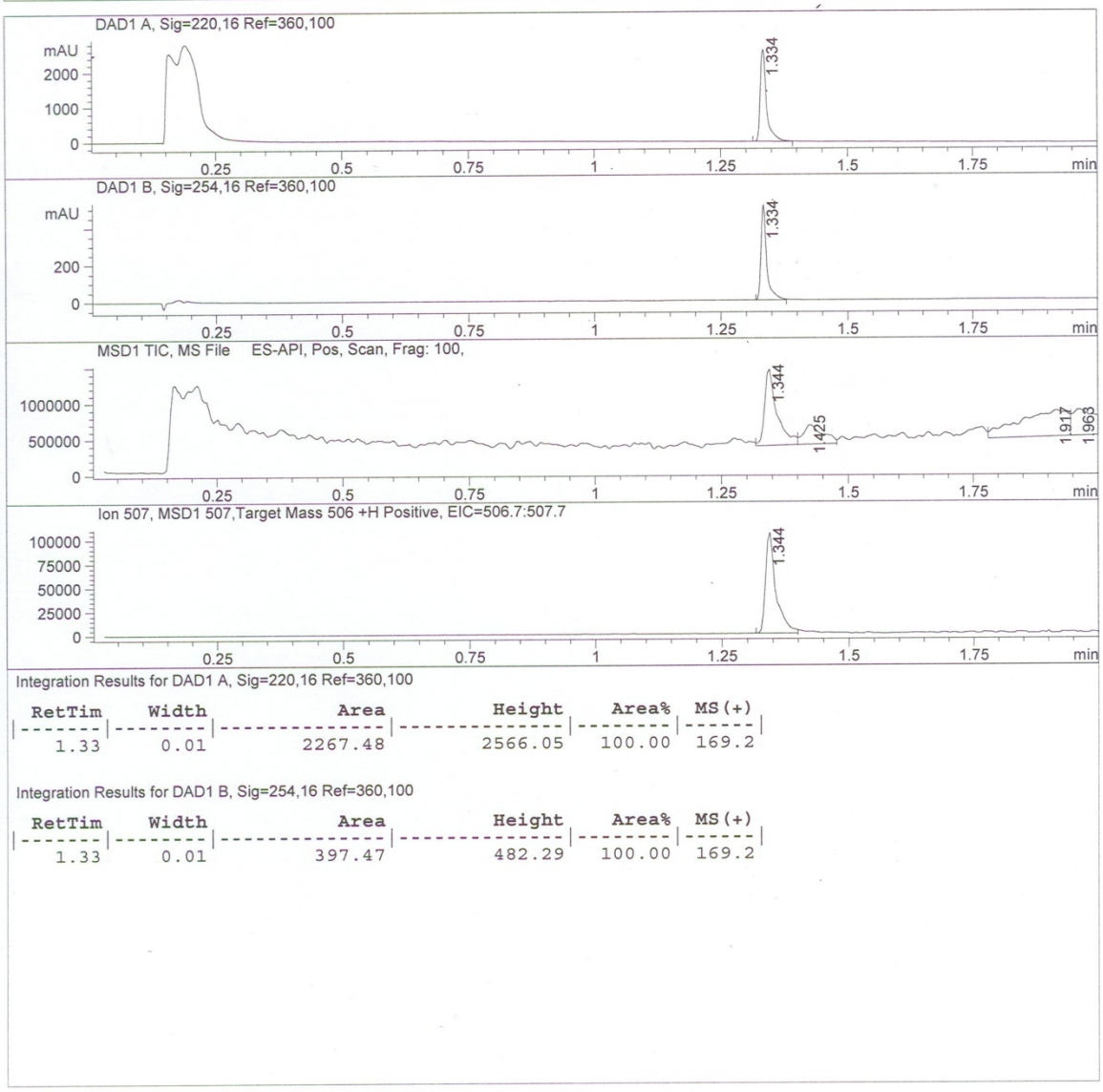

Integration Results for DAD1 A, Sig=220,16 Ref=360,100

RetTim	Width	Area	Height	Area%	MS(+)
1.33	0.01	2267.48	2566.05	100.00	169.2

Integration Results for DAD1 B, Sig=254,16 Ref=360,100

RetTim	Width	Area	Height	Area%	MS(+)
1.33	0.01	397.47	482.29	100.00	169.2

MS Report

Ret. Time: 1.34 <<<< POSITIVE SPECTRA >>>> Ret. Time: 1.43

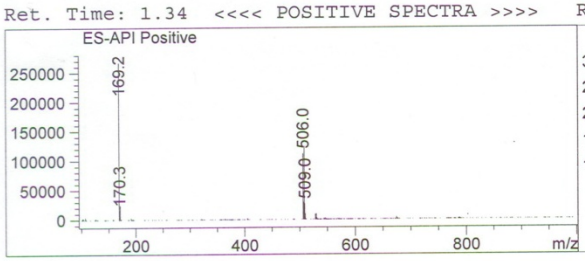

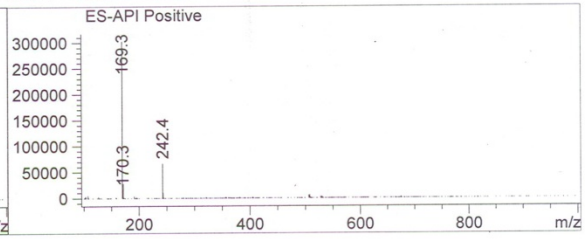

Ret. Time: 1.92 Ret. Time: 1.96

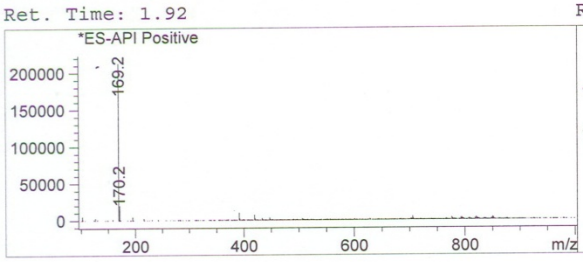

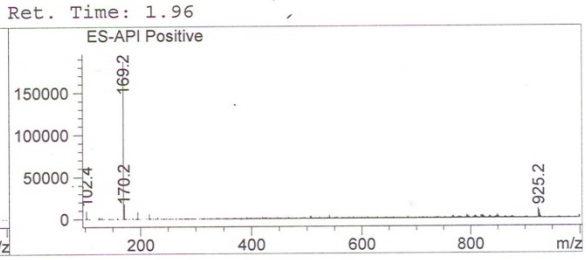

Elemental Composition Report

Single Mass Analysis

Tolerance = 5.0 PPM / DBE: min = 0.0, max = 25.0
Element prediction: Off
Number of isotope peaks used for i-FIT = 2

Monoisotopic Mass, Even Electron Ions
356 formula(e) evaluated with 1 results within limits (up to 50 closest results for each mass)
Elements Used:
C: 20-500 H: 1-1000 N: 1-200 O: 1-200 S: 1-1 Br: 1-1 F: 1-1

VU0405652

S/N: UH193

18-Mar-2010
13:50:44
1: TOF MS ES+
2.13e+003

031710_mjm_003 117 (1.296) AM (Cen,4, 80.00, Ar,8000.0,556.28,0.70,LS 5); Sm (SG, 2x1.00); Cm (115:117)

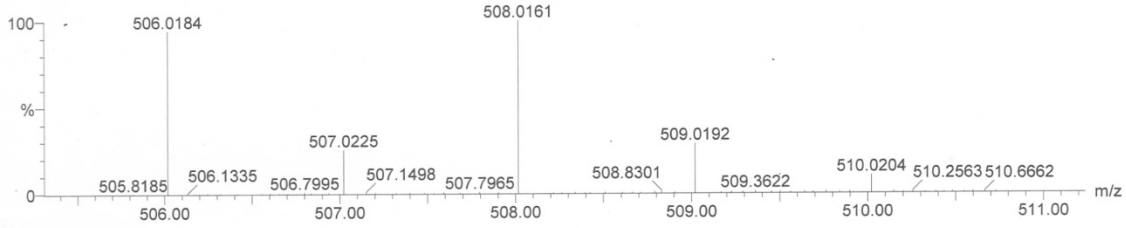

Minimum:				0.0		
Maximum:		5.0	5.0	25.0		
Mass	Calc. Mass	mDa	PPM	DBE	i-FIT	Formula
506.0184	506.0185	-0.1	-0.2	13.5	0.4	C21 H18 N3 O4 S Br F

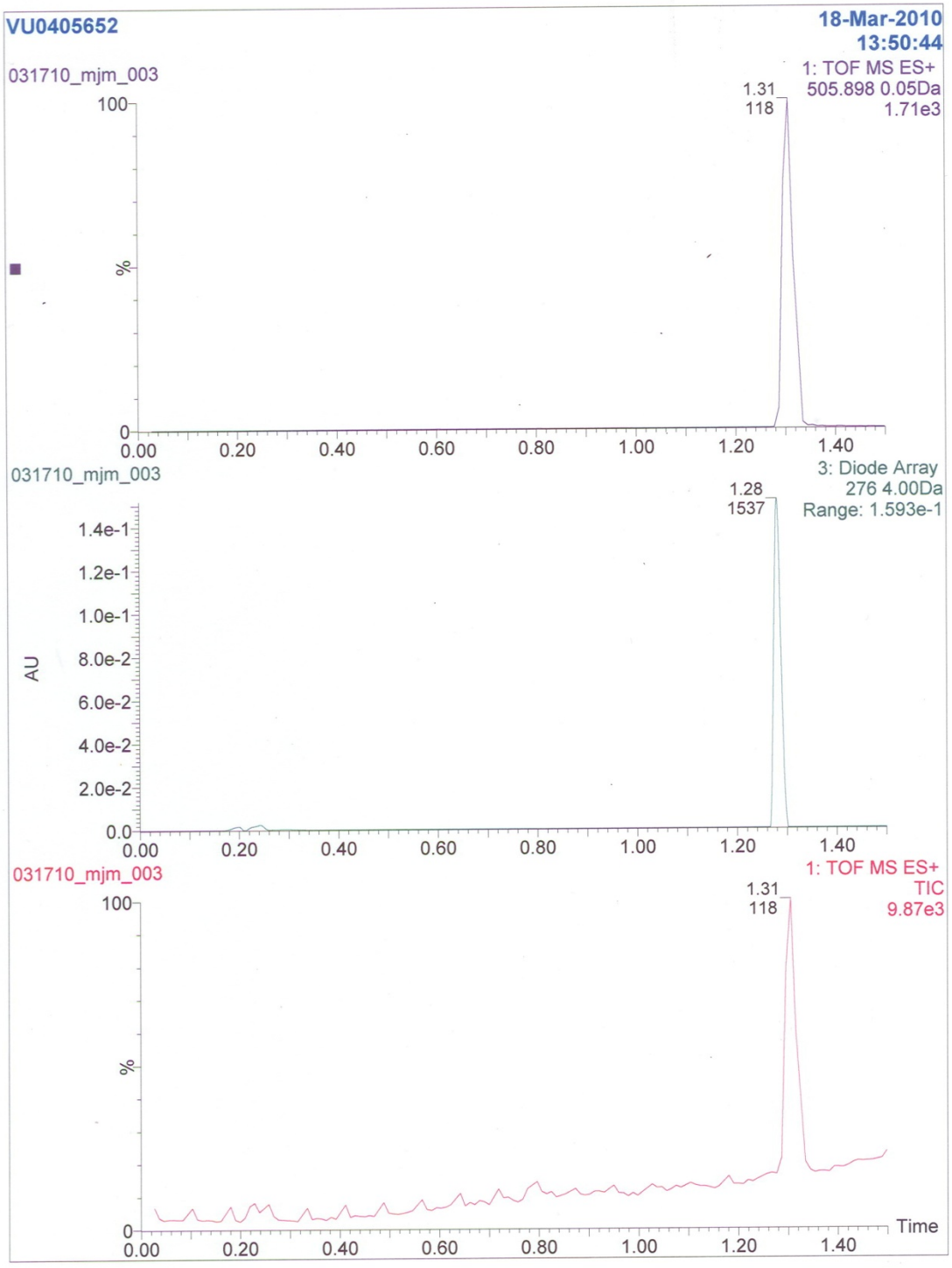
VU0405652
18-Mar-2010
13:50:44
031710_mjm_003
1: TOF MS ES+
505.898 0.05Da
1.71e3
1.31
118
100
%
0
0.00
0.20
0.40
0.60
0.80
1.00
1.20
1.40
031710_mjm_003
3: Diode Array
276 4.00Da
Range: 1.593e-1
1.28
1537
AU
1.4e-1
1.2e-1
1.0e-1
8.0e-2
6.0e-2
4.0e-2
2.0e-2
0.0
031710_mjm_003
1: TOF MS ES+
TIC
9.87e3
1.31
118
Time

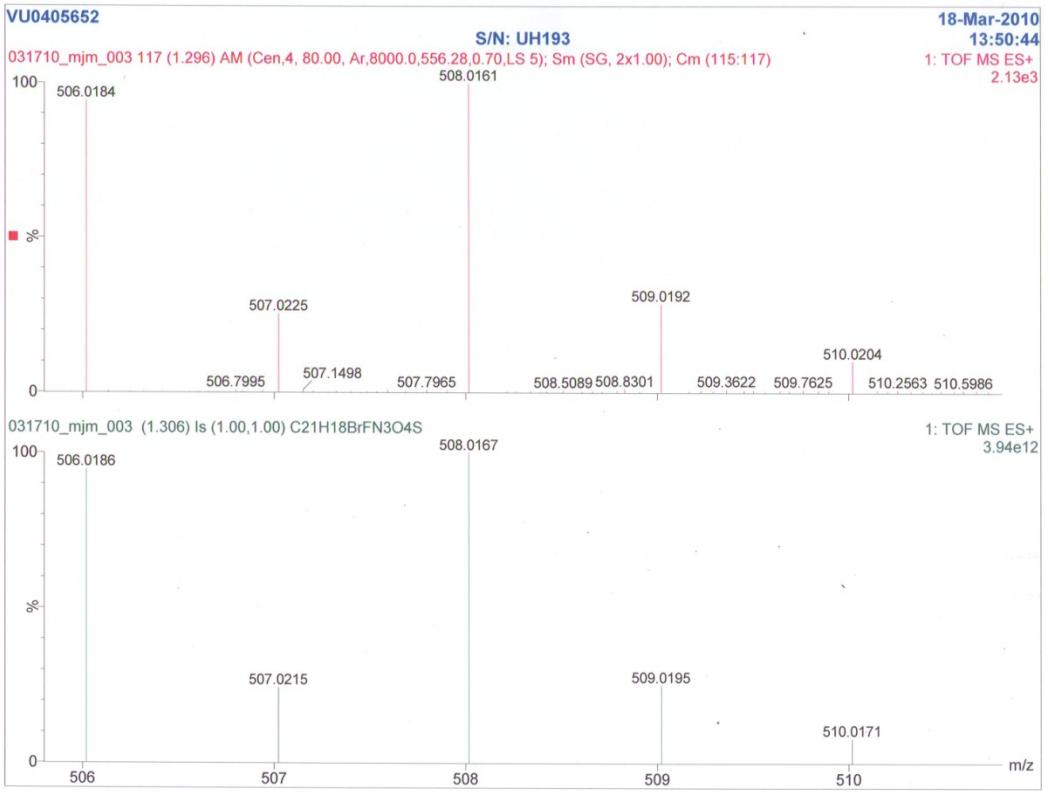
VU0405652
S/N: UH193
18-Mar-2010
13:50:44
031710_mjm_003 117 (1.296) AM (Cen,4, 80.00, Ar,8000.0,556.28,0.70,LS 5); Sm (SG, 2x1.00); Cm (115:117)
1: TOF MS ES+
2.13e3
100
%
0
506.0184
508.0161
507.0225
509.0192
510.0204
506.7995
507.1498
507.7965
508.5089
508.8301
509.3622
509.7625
510.2563
510.5986
031710_mjm_003 (1.306) Is (1.00,1.00) C21H18BrFN3O4S
1: TOF MS ES+
3.94e12
100
%
0
506.0186
508.0167
507.0215
509.0195
510.0171
m/z
506
507
508
509
510